Monthly Notices of the ROYAL ASTRONOMICAL SOCIETY

MNRAS **438,** 789–795 (2014)
Advance Access publication 2013 December 13

doi:10.1093/mnras/stt2248

BOKS 45906: a CV with an orbital period of 56.6 min in the *Kepler* field?

Gavin Ramsay,[1★] Steve B. Howell,[2,3] Matt A. Wood,[4] Alan Smale,[5] Thomas Barclay,[2,6] Sally A. Seebode,[3,7] Dawn Gelino,[3,8] Martin Still[2,5] and John K. Cannizzo[9,10]

[1]*Armagh Observatory, College Hill, Armagh BT61 9DG, UK*
[2]*NASA Ames Research Center, Moffett Field, CA 94095, USA*
[3]*Visiting Astronomer, Mt. Palomar Observatory, Palomar Mt, CA 92060, USA*
[4]*Physics & Astronomy Department, Texas A&M University-Commerce, Commerce, TX 75429, USA*
[5]*NASA/Goddard Space Flight Center, Greenbelt, MD 20771, USA*
[6]*Bay Area Environmental Research Institute, Inc., 560 Third St. West, Sonoma, CA 95476, USA*
[7]*San Mateo High School, San Mateo, CA 94401, USA*
[8]*NASA Exoplanet Science Institute, Caltech, Pasadena, CA 91125, USA*
[9]*CRESST and Astroparticle Physics Laboratory NASA/GSFC, Greenbelt, MD 20771, USA*
[10]*Department of Physics, University of Maryland, Baltimore County, 1000 Hilltop Circle, Baltimore, MD 21250, USA*

Accepted 2013 November 17. Received 2013 November 17; in original form 2013 October 29

ABSTRACT

BOKS 45906 was found to be a blue source in the Burrell-Optical-Kepler Survey which showed a 3 mag outburst lasting ∼5 d. We present the *Kepler* light curve of this source which covers nearly 3 years. We find that it is in a faint optical state for approximately half the time and shows a series of outbursts separated by distinct dips in flux. Using data with 1 min sampling, we find clear evidence that in its low state BOKS 45906 shows a flux variability on a period of 56.5574 ± 0.0014 min and a semi-amplitude of ∼3 per cent. Since we can phase all the 1 min cadence data on a common ephemeris using this period, it is probable that 56.56 min is the binary orbital period. Optical spectra of BOKS 45906 show the presence of Balmer lines in emission indicating it is not an AM CVn (pure Helium) binary. *Swift* data show that it is a weak X-ray source and is weakly detected in the bluest of the UVOT filters. We conclude that BOKS 45906 is a cataclysmic variable with a period shorter than the 'period-bounce' systems and therefore BOKS 45906 could be the first helium-rich cataclysmic variable detected in the *Kepler* field.

Key words: binaries: close – stars: dwarf novae – stars: individual: BOKS 45906 – novae, cataclysmic variables.

1 INTRODUCTION

Cataclysmic variables (CVs) are binary systems which contain a white dwarf primary star that accretes material from a Roche lobe-filling late-type main-sequence secondary star. The secondary star's surface contacts its Roche lobe through angular momentum loss and initiates ballistic mass transfer to the white dwarf through the inner Lagrange point L_1. The mass transfer that occurs at this point is mostly stable and causes the '*cataclysmic*' phenomenon. If the white dwarf retains enough of the accreted material, it can exceed the Chandrasekhar limit and become a Type Ia supernova. Thus, CVs have a broad importance for studying the physics of the accretion process in detail, and in constraining models of stellar evolution, binary evolution, and the chemical enrichment of the Galaxy.

Although CVs have been observed for more than 100 years (e.g. Cannizzo 2012), *Kepler* provided essentially uninterrupted observations of sources for months or years which allowed the outburst properties of CVs to be studied in a way not previously possible. Since the launch of *Kepler*, we have pursued a programme to study a range of CVs in the *Kepler* field of view (there are several dozen; see Howell et al. 2013; Scaringi, Groot & Still 2013, for details). A brief overview of our work can be found in Ramsay et al. (2012). Other groups which have published recent work on *Kepler* CVs include Scaringi et al. (2013), Kato & Maehara (2013), Gies et al. (2013) and Osaki & Kato (2013).

One source in the *Kepler* field, BOKS 45906 [KIC 9778689, $\alpha = 19^{\rm h}40^{\rm m}16\overset{\rm s}{.}2$ $\delta = +46^\circ32'47\overset{''}{.}9$ J2000.0, taken from the Kepler Isaac Newton Telescope (INT) Survey], was identified as a blue source in the Burrell-Optical-Kepler Survey (BOKS) which was a pre-launch survey of the central region of the *Kepler* field of view. BOKS 45906 was seen to undergo what appeared to be a typical

★ E-mail: gar@arm.ac.uk

© 2013 The Authors
Published by Oxford University Press on behalf of the Royal Astronomical Society

Downloaded from http://mnras.oxfordjournals.org/ at NASA Goddard Space Flight Ctr on September 5, 2014

dwarf nova outburst, rising from a quiescent magnitude of $R = 20$ to 16.5 and lasting for about 5 d. A subsequent study by Howell (unpublished) over the past few years has shown BOKS 45906 to reside near $V = 22.5$ and no further outbursts such as detected by Feldmeier et al. (2011) have been noted. There is a faint X-ray source (0.02 count s^{-1}) detected in *ROSAT* All-Sky Faint Survey Catalogue (Voges et al. 1999) which is 3.5 arcsec distant from the optical position of BOKS 45906.

As part of a broader programme to study CVs (and accreting objects in general) in NASA's *Kepler* field of view, we added BOKS 45906 to our *Kepler* programme. In this paper we present the *Kepler* data of BOKS 45906 with additional data obtained using the INT, *Swift* and the Hale 200 inch Telescope, and discuss their likely nature.

2 OPTICAL COLOURS

The *Kepler INT Survey* (KIS; Greiss et al. 2012a,b) obtained $Ugri$H$_\alpha$ photometry of the vast majority of sources in the *Kepler* field. The photometry and colours of BOKS 45906 are $g = 19.85$, $U - g = -1.24$, $g - r = 0.44$, $r - i = 0.42$ and r −Hα = 1.22 indicating it has colours consistent with those of CVs (Fig. 1). The *Kepler* data imply that these KIS observations took place when the source was in a high optical state (Section 3). Although the KIS multi-colour observations took place within 8 min of each other, our INT observations (cf. Section 4) indicate that some degree of caution should be taken since it can change brightness by up to 0.4 mag on this time-scale.

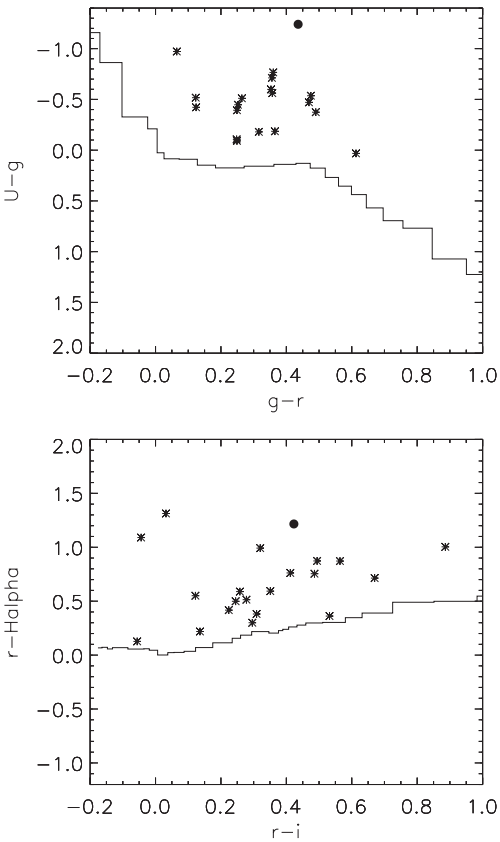

Figure 1. The colours of BOKS 45906 (the filled circle) in the $U - g$, $g - r$ (top panel) and the $r - i$, r −Hα (lower panel). We show the track of the unreddened main sequence taken from Groot et al. (2009) (top) and Drew et al. (2005) (bottom). We also show the colours of known CVs in the *Kepler* field (taken from Scaringi et al. 2013; Howell et al. 2013).

3 KEPLER PHOTOMETRIC OBSERVATIONS

3.1 Analysis of the *Kepler* data

The detector on board *Kepler* is a shutterless photometer using 6 s integrations and a 0.5 s readout. There are two modes of observation: *long cadence* (LC), where 270 integrations are summed for an effective 29.4 min exposure (this includes deadtime), and *short cadence* (SC), where nine integrations are summed for an effective 58.8 s exposure. Gaps in the *Kepler* data streams result from, for example, 90° spacecraft rolls every 3 months (called Quarters), and monthly data downloads using the high gain antenna.

Kepler data are available in the form of FITS files which are distributed by the Mikulski Archive for Space Telescope (MAST).[1] For LC data each file contains one observing quarter worth of data whereas for SC data one file is created per month. After the raw data are corrected for bias, shutterless readout smear, and sky background, time series are extracted using simple aperture photometry (SAP). The start and end times of each quarter of *Kepler* data which are used in this study are shown in Table 1. SC mode data were obtained in Q6–8, 11 and 15. (We note that when SC data are obtained, LC data are also produced.) BOKS 45906 is located in a relatively crowded field ($b = 11\overset{\circ}{.}6$). There is a faint ($g = 21.8$) star 8.9 arcsec to the NW of BOKS 45906 and a brighter ($g = 18.3$) star 13.0 arcsec also to the NW of BOKS 45906 (these can be seen in Fig. 2) where the source magnitudes come from the *Kepler INT Survey* (Greiss et al. 2012a,b). Using the PyKe software,[2] we find that the brighter of these two stars is likely to contaminate the standard photometric results of BOKS 45906 (*Kepler* pixels are 3.98 arcsec^2). We therefore used the PyKe tasks KEPPIXSERIES, KEPMASK and KEPEXTRACT to extract photometric data from one pixel which clearly showed the presence of BOKS 45906 in all quarters of data.

Data which were not flagged as 'SAP_QUALITY = 0' in the FITS files were removed (for instance, time intervals of enhanced solar activity). When BOKS 45906 was in a low optical state, we corrected for systematic trends (Kinemuchi et al. 2012). (In a high optical state this 'correction' introduced spurious effects). Due to the rotation of the spacecraft the source lies on a different chip each quarter. We therefore applied a small correction to the resulting flux so that there were no discrete jumps in the light curve from quarter to quarter. We show the resulting light curve binned into 1 d means in Fig. 3.

3.2 Overall characteristics of the light curve

The SC light curve for quarters Q6–Q8 was presented initially in Howell et al. (2013). In their paper, BOKS 45906 was seen to be in a low state with only a few low-amplitude flare-like events noted. The LC *Kepler* light curve now covers 1018 d (2.8 yr). For the first year of observation, BOKS 45906 was typically in a low state, with occasional short-duration flux enhancements. However, at MJD∼55752 there is a rapid (∼2 d) increase in the flux (a factor of 5.7, or 1.9 mag) of BOKS 45906. Over the next ∼145 d the flux gradually decreases until it makes a rapid ∼2–3 d descent back to its

[1] http://archive.stsci.edu/kepler
[2] http://keplergo.arc.nasa.gov/PyKE.shtml

Downloaded from http://mnras.oxfordjournals.org/ at NASA Goddard Space Flight Ctr on September 5, 2014

Table 1. Journal of *Kepler* observations. The start and end MJD and UT dates are the mid-point of the first and final cadence of the LC time series for each quarter, respectively.

Quarter	Start		End	
	MJD	UT	MJD	UT
Q6 (LC)	55371.947	2010 Jun 24 22:46	55461.794	2010 Sept 22 19:04
Q7 (LC)	55462.673	2010 Sept 23 16:10	55552.049	2010 Dec 22 01:09
Q8 (LC)	55567.865	2011 Jan 06 20:45	55634.846	2011 Mar 14 20:18
Q9 (LC)	55641.017	2011 Mar 21 00:24	55738.424	2011 Jun 26 10:10
Q10 (LC)	55739.343	2011 Jun 27 08:16	55832.766	2011 Sept 28 18:24
Q11 (LC)	55833.706	2011 Sept 29 16:56	55930.827	2012 Jan 04 19:50
Q12 (LC)	55931.910	2012 Jan 05 21:50	56014.523	2012 Mar 28 12:33
Q13 (LC)	56015.238	2012 Mar 27 05:42	56105.554	2012 Jun 27 13:17
Q14 (LC)	56106.637	2012 Jun 28 15:17	56203.820	2012 Oct 03 19:40
Q15 (LC)	56205.985	2012 Oct 05 23:38	56303.638	2013 Jan 11 15:18
Q16 (LC)	56304.598	2013 Jan 12 14:21	56390.460	2013 Apr 08 11:02
Q6-1 (SC)	55371.937	2010 Jun 24 22:29	55399.032	2010 Jun 24 22:29
Q6-2 (SC)	55399.870	2010 Jul 22 20:53	55430.786	2010 Jul 22 20:53
Q6-3 (SC)	55431.685	2010 Aug 23 16:26	55461.804	2010 Aug 23 16:26
Q7-1 (SC)	55462.663	2010 Sept 23 15:54	55492.781	2010 Sept 23 15:54
Q7-2 (SC)	55493.538	2010 Oct 24 12:54	55522.737	2010 Oct 24 12:54
Q7-3 (SC)	55523.616	2010 Nov 23 14:47	55552.059	2010 Nov 23 14:47
Q8-1 (SC)	55567.855	2011 Jan 06 20:30	55585.550	2011 Jan 06 20:30
Q8-2 (SC)	55585.612	2011 Jan 24 14:40	55614.708	2011 Jan 24 14:40
Q8-3 (SC)	55614.770	2011 Feb 22 18:29	55634.856	2011 Feb 22 18:29
Q11-1 (SC)	55833.700	2011 Sept 29 16:42	55864.775	2011 Sept 29 16:42
Q11-2 (SC)	55865.531	2011 Oct 31 12:45	55895.732	2011 Oct 31 12:45
Q11-3 (SC)	55896.611	2011 Dec 01 14:39	55930.837	2011 Dec 01 14:39
Q15-1 (SC)	56205.976	2012 Oct 05 23:24	56236.809	2012 Oct 05 23:24
Q15-2 (SC)	56237.770	2012 Nov 06 18:29	56267.889	2012 Nov 06 18:29
Q15-3 (SC)	56268.727	2012 Dec 07 17:27	56303.648	2012 Dec 07 17:27

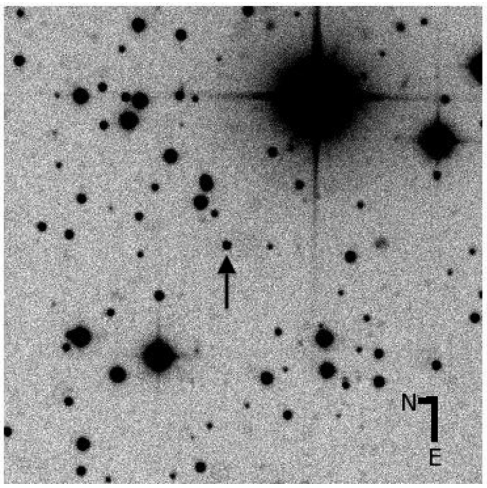

Figure 2. The finding chart of BOKS 45906 (marked by an arrow) made using the INT in 2013 July. It was made by combining 11 separate *g*-band images, the effective exposure being 660 s. The image is 2 arcmin across.

'quiescent' state. However, it only remains in a quiescent state for ∼10 d, thereafter showing short-duration events for the next ∼280 d going into a series of bright states interspersed with 'dips' in the light curve which have sharp ingress and egrees features when the source returns to its quiescent flux. The last 100 d of the light curve show it in a quiescent state apart from one short-duration event. The fact that the flux returns to quiescence after the initial long outburst (and the following outbursts) makes it different in character to the 'echo' outbursts seen in WZ Sge (e.g. Patterson et al. 2002).

3.3 A search for short-period variations

SC data with an effective exposure of 58.85 s were obtained in five quarters, Q6, Q7, Q8, Q11 and Q15 (see Table 1). We removed data from time intervals of enhanced solar background in a similar way to the LC analysis, and we used the pixel level data and extracted light curves using the one pixel that BOKS 45906 was most strongly detected on.

For the Q6-1 data we first removed data from the time interval where there was a flux enhancement lasting ∼2 d. The mean count for this resulting light curve (Fig. 4) was 29.6 count s^{-1} with a standard deviation (rms) of 6.3 count s^{-1} (21 per cent). In contrast, the pixel corresponding to 319 991 in the KEPPIXSERIES map, which we took to represent the background, gave a mean flux of −0.3 count s^{-1} indicating that BOKS 45906 was clearly detected. The Lomb Scargle Power Spectrum of the Q6-1 light curve of BOKS 45906 is shown in Fig. 5 and indicates a very prominent peak at a period of 56.56 min.

Although there is no previously known spurious period caused by instrumental effects at 56.56 min, we note it is close to twice the effective exposure of the LC data (58.867 min). We therefore searched for a periodic signal in all of the other pixels in the Q6 data and found evidence for this period in only three other pixels which were adjacent to the pixel where BOKS 45906 was most strongly detected. In addition we also extracted the RAW_FLUX data (i.e. using the original data which have not been corrected for flat-fielding, etc.) and find evidence for a period of 56.56 min in the same three pixels and none of the others.

For all of the other SC data we extracted the light curve for BOKS 45906 in the same manner and removed data from those time intervals where the source was in a brighter optical state. We

Downloaded from http://mnras.oxfordjournals.org/ at NASA Goddard Space Flight Ctr on September 5, 2014

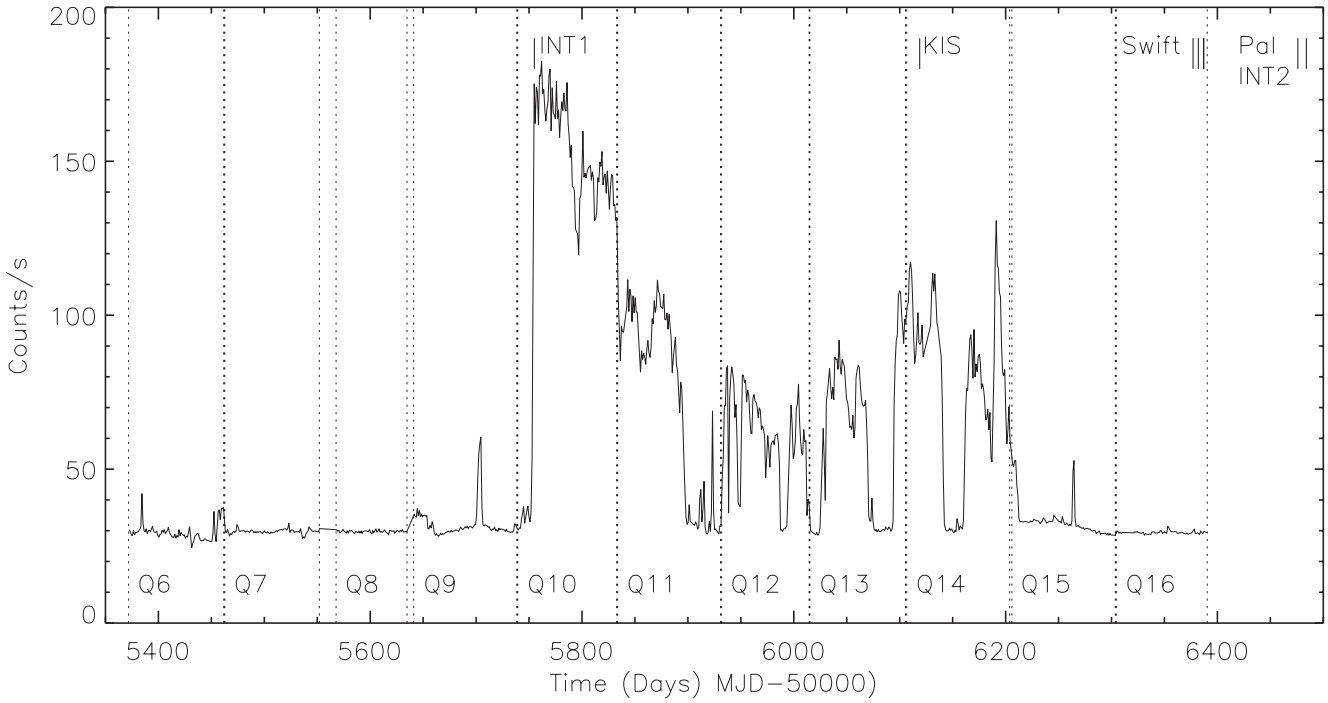

Figure 3. The *Kepler* LC *Kepler* light curve of BOKS 45906 which covers Q6–16 binned into 1 d bins. The time unit is in MJD - 50000.0. We mark the dates when INT, KIS, *Swift* and Palomar (Pal) observations were made.

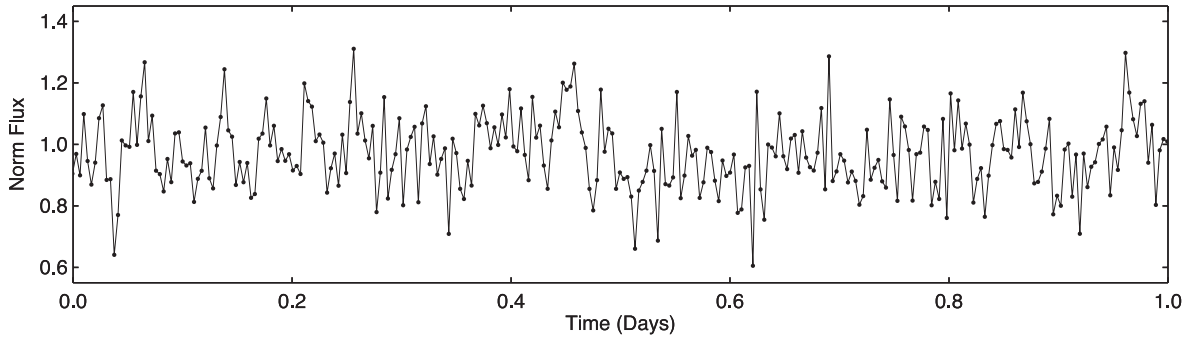

Figure 4. The light curve of BOKS 45906 using SC data from Q6-1 where we have binned the data into 5 min bins and show only 1 d of data. The data have been normalized so that the mean flux is set at unity.

find each quarter of data has a strong peak in the corresponding Lomb Scargle Power Spectra at 56.56 min. Taking all of these data we find a period of 56.55804 min (we show the Lomb Scargle Power spectra of all low state data in Fig. 5.). We find that the following ephemeris:

$$T_o = \text{HJD245 5372.4512(5)} + 0.039276(1)E \quad (1)$$

can phase each of the low optical state data sets so that the minimum corresponds to $\phi = 0.0$ (Fig. 6). (The error on the folding epoch was derived from the mean error on the phase of the flux minimum in the folded light curves and the error on the period is the full-width-half-maximum of the main peak in the power spectrum shown in Fig. 5.) We fitted a sine wave to each of these folded light curves and show the best fit and error of the half-amplitude for each epoch in Fig. 6. We find that the mean half-amplitude is 3.3 per cent which is much smaller than the rms of the Q6-1 light curve (21 per cent). Given the stable nature of this period we suggest that the period of 56.56 min represents the orbital period of this system.

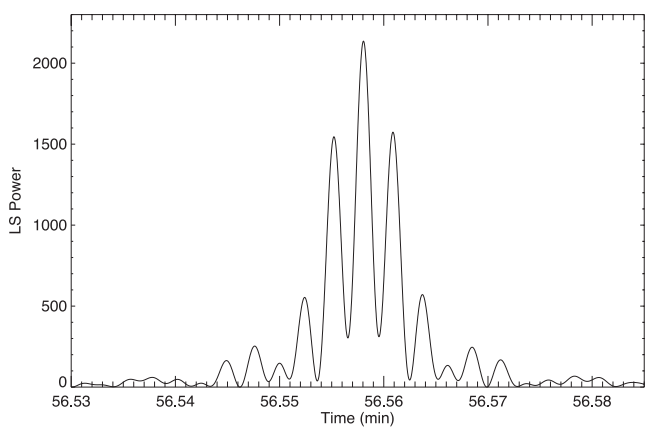

Figure 5. The Lomb Scargle Power Spectrum of BOKS 45906 using SC data from Q6, 7, 8 and 15 when the BOKS 45906 was in a low state. There is a very strong peak in the power spectrum corresponding to a period of 56.557 min.

Downloaded from http://mnras.oxfordjournals.org/ at NASA Goddard Space Flight Ctr on September 5, 2014

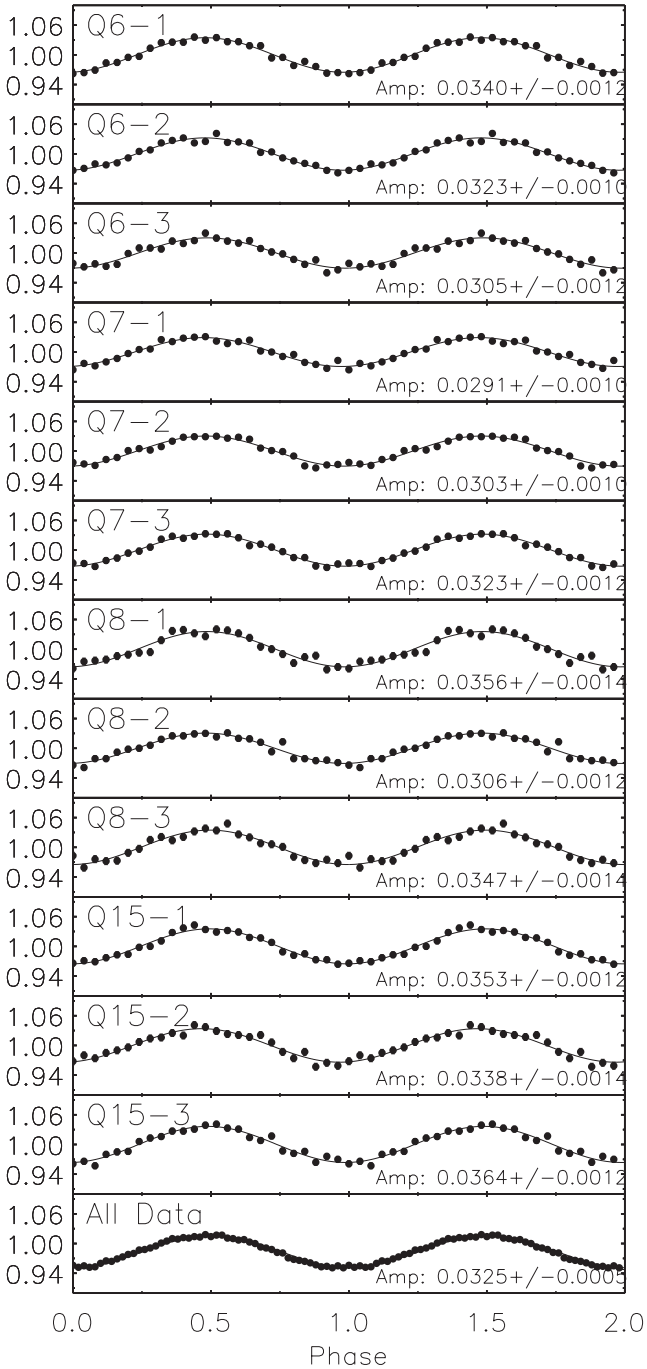

Figure 6. The SC data of BOKS 45906 folded on a period of 56.55804 min with phase zero being HJD 2455 5372.4512.

We also searched for the presence of the 56.56 min period when the system was in a high optical state: it was detected at a much lower significance even in the high state data. The power spectra of the high state data are complex with peaks corresponding to periods of ∼0.1–0.3 d.

4 GROUND-BASED PHOTOMETRY

We observed BOKS 45906 using the 2.5 m INT, located on the island of La Palma, on 2011 July 13 and again on 2013 July 11 as part of the *RATS-Survey* (Ramsay et al. 2013). The Wide Field Camera

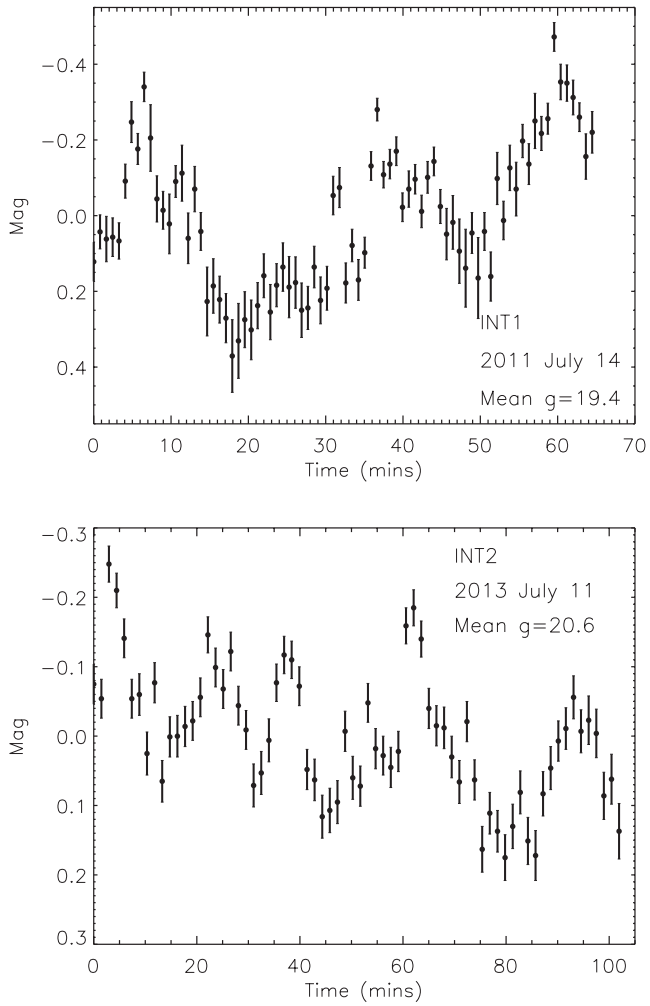

Figure 7. Light curves of BOKS 45906 obtained using the INT in 2011 July (top) when the source was in a bright optical state and in 2013 July (bottom) when the source was in a faint optical state.

was used with a g-band filter. The 2011 observations were made using a 20 s exposure and the light curve (Fig. 7) covered 65 min and the source had a mean brightness of $g = 19.4$ (using the KIS to determine the brightness of nearby comparison stars) although BOKS 45906 reached a peak of $g = 18.8$ during these observations. Although the source is obviously variable, there is no clear periodic signal. In contrast the 2013 observations were made when the source was in a low state ($g = 20.6$) and exposures were 60 s in duration. Although there are clear short time-scale variations (lower panel Fig. 7) there is no periodic signal. The standard deviation of this light curve is 0.09 mag which is greater than the 3 per cent semi-amplitude modulation of the 56.56 min period seen in the *Kepler* SC data. It is therefore no surprise that we do not detect the 56.56 min period in these short-duration light curves.

5 OPTICAL SPECTROSCOPY

We used the 200 inch Hale Telescope on Palomar Mountain, California, and the double beam spectrograph (DBS) to obtain a small number of optical spectra of BOKS 45906. The DBS has an intensified CCD acquisition camera which can be used to take timed exposures of the local field of view which helps to find and

Downloaded from http://mnras.oxfordjournals.org/ at NASA Goddard Space Flight Ctr on September 5, 2014

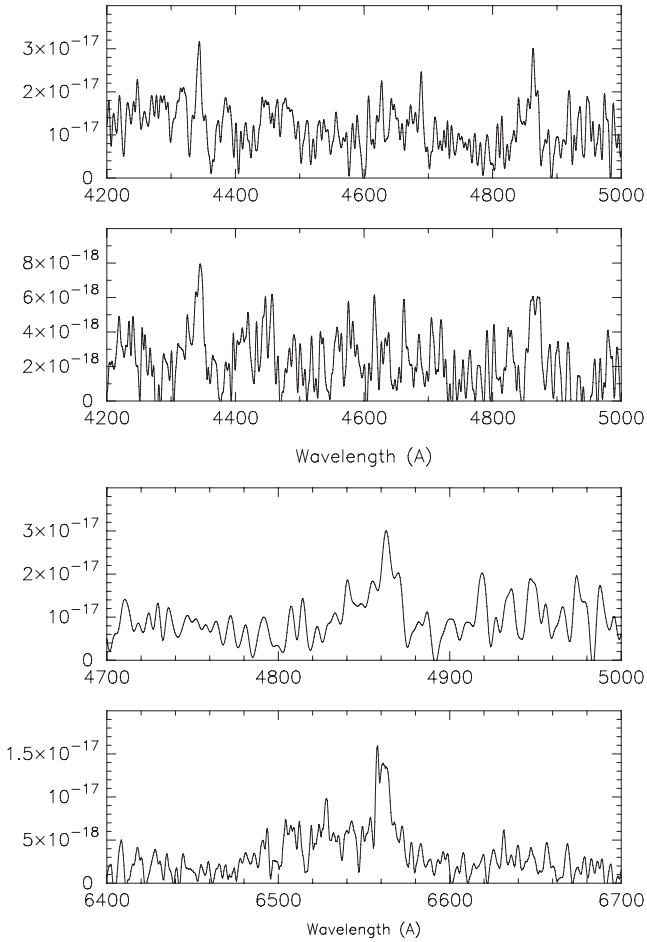

Figure 8. The upper two panels show our first and second blue spectra covering Hβ through Hδ (the flux scale is in erg s^{-1} cm^{-2} Å^{-1}). The Balmer emission lines as well as the continuum level weakened in the second and subsequent exposures. The bottom two panels show regions centred on Hβ and Hα from the first spectrum pair. BOKS 45906 was at minimum light during these observations.

place faint sources on the slit. We obtained a sequence of four 20-min exposures of BOKS 45906 on 2013 July 2 starting at 09:38 UT. Observations made using the INT (Section 4) 9 d after these observations show BOKS 45906 to be in a low but variable optical state.

The D-55 dichroic filter was used to split light between the blue and red arms. The blue arm used a 1200 lines mm^{-1} grating providing of resolution of $R \sim 7700$ and covered 1500 Å in wavelength. The red arm used a 1200 lines mm^{-1} grating providing a resolution of $R \sim 10000$ and a wavelength coverage of 670 Å. The slit width was set to 1 arcsec and the usual procedures of observing spectrophotometric standard stars and arc lamps were adhered to. Red and blue spectra were wavelength calibrated using a HeNeAr and FeAr arc-lamp, respectively. The night was clear and provided stable seeing near 1 arcsec. Data reduction was done using IRAF 2D and 1D routines for spectroscopic data and produced a final 1D spectrum for each observation.

Fig. 8 shows the Balmer lines for the first blue and red pair as well as a comparison of the first two blue spectra. During the sequence of the four spectra we obtained, the star brightness dropped by 30 per cent in flux from exposure 1 to 2 and continued to drop during the remaining two exposures, being only 1/4 as bright during the last exposure. Based on the slit viewer camera, BOKS 45906 was estimated to be near $V = 22$ during the observations. Due to this rapid dimming during the four exposures, the final three red spectra and the final two blue spectra are very low signal-to-noise ratio (S/N), showing weak emission in a rather noisy continuum. We cannot reliably measure the line centre or line flux changes in the last three spectra due to the faintness of the star. The spectra do, however, confirm that BOKS 45906 is an emission line source, rapidly variable, and shows a flat Balmer decrement.

Table 2. Details of the *Swift* UVOT observations where we indicate the ObsId; start date of the observations; which filter was being used and the detected flux.

ObsID	Start date (MJD)	UVOT filter	Flux erg s^{-1} cm^{-2}Å^{-1}
00032763001	56377.55	UVW2	$1.2 \pm 0.2 \times 10^{-17}$
00032763002	56382.03	UVM2	-
00032763003	56387.33	UVW1	-
00032763004	56392.52	U	-

6 *SWIFT* OBSERVATIONS

We obtained target of opportunity observations of BOKS 45906 using the NASA *Swift* satellite (Gehrels et al. 2004) at four epochs separated by ~5 d. As can be seen from Fig. 3 they were made when the source was in a low optical state. Because *Swift* is in a low Earth orbit, each observation sequence (which makes up an 'ObservationID') is made up of typically two to four separate pointings. The exposure time of each UVOT image is generally 1200 s in duration, while the total exposure time of the X-ray observation in each ObservationID is typically 3–4 ks. Observations commenced on 2013 March 26. See Table 2 for the start date of each observation.

6.1 XRT observations

The X-ray Telescope (XRT; Burrows et al. 2005) on-board *Swift* has a field of view of 23.6 × 23.6 arcmin with CCD detectors. It is sensitive over the range 0.2–10 keV and has an effective area of ~70 cm^2 at 1 keV (for comparison the *ROSAT* XRT had an effective area of ~400 cm^2 at 1 keV). We examined data taken in 'photon counting' mode and used the products derived from the standard XRT pipeline.

Since the count rate of BOKS 45906 was low we created an image using all the XRT data in photon counting mode. This image was input to the HEASOFT tool XIMAGE and the routine SOSTA (which takes into account effects such as vignetting, exposure and the point spread function) to determine the count rate and error at the optical position of BOKS 45906. The total exposure was 14.1 ks and the count rate was $6.2 \pm 3.1 \times 10^{-4}$ count s^{-1} giving a S/N of 2.0. It was therefore detected at a low significance.

6.2 UVOT observations

The Ultra-Violet/Optical Telescope (UVOT) on board the *Swift* satellite has a 30 cm primary mirror and six optical/UV filters (Roming 2005). Since *Swift* operates a 'filter of the day', we were not able to pre-define the filter, but images were obtained in the U (central wavelength 347 nm, and a full width half-maximum of 79 nm), UVW1 (251 nm, 70 nm), UVM2 filter (225 nm, 50 nm) and the UVW2 (188nm, 76 nm) filters. BOKS 45906 was detected only

Downloaded from http://mnras.oxfordjournals.org/ at NASA Goddard Space Flight Ctr on September 5, 2014

in the UVW2 filter (the filter with the bluest response) and then at a very low count rate: 0.020 ± 0.003 count s^{-1} which corresponds to a flux of $1.23 \pm 0.21 \times 10^{-17}$ erg s^{-1} cm^{-2} $Å^{-1}$.

7 DISCUSSION

The *Kepler* observations of BOKS 45906 cover a time interval of nearly 3 years during which its optical flux varies by a factor of ∼6. This together with the fact that it is detected as a very weak X-ray and UV source, and shows Balmer emission lines, all point to the fact that BOKS 45906 is an accreting source. During the low optical state there is a strong peak in the power spectrum corresponding to a period of 56.56 min. Given that we can phase all of the *Kepler* SC data on a common ephemeris, this strongly suggests that 56.56 min is the orbital period of an accreting binary system (other periods which may be expected, such as a super-hump period, would not be expected to be as stable).

As CVs evolve over time their orbital period decreases due to the loss of orbital angular momentum from the system. However, at some point, the mass of the secondary star becomes so small that hydrogen burning in the core stops and it becomes semi-degenerate. The radius of the secondary will thereafter start to increase and the orbital period starts to increase again. This period 'bounce' is predicted to occur at ∼65–70 min (Rappaport, Joss & Webbink 1982; Kolb & Baraffe 1999; Howell, Nelson & Rappaport 2001), and is observed at ∼80 min (Gänsicke et al. 2009).

There are, however, two groups of helium-rich accreting binary systems which have orbital periods shorter than 70 min. The 'AM CVn' binaries have orbital periods between ∼5 and 70 min and spectra devoid of hydrogen. Given we detect Balmer lines in its spectrum, BOKS 45906 cannot be an AM CVn system. A much smaller group of accreting binaries is also known which shows strong helium and hydrogen lines and also show outbursts (e.g. Breedt et al. 2012; Carter et al. 2013). It is thought that these 'helium-rich' binaries may evolve to become AM CVn systems over time. Although our optical spectra have low S/N we do not see any clear evidence for helium lines. However, other CVs below the period minimum such as EI Psc which has an orbital period of 64 min (Thorstensen et al. 2002) show relatively weak helium emission lines, which could well be hidden in low S/N spectra.

Breedt et al. (2012) give an overview of the accreting binaries with an orbital period less than 76 min. Of the 42 then-known systems, 36 of these are AM CVn binaries and three are confirmed (and another three candidate) hydrogen accreting systems. Finding another candidate hydrogen accreting binary with an orbital period less than 76 min is clearly of great interest from a binary evolutionary point of view. The next step is to obtain time-resolved spectra of BOKS 45906 when it is in a bright optical state to confirm that 56.56 min is indeed the binary orbital period.

8 CONCLUSIONS

We have identified one object in the *Kepler* field, BOKS 45906, which shows a series of outbursts which can reach ∼2 mag in amplitude. Using SC data when the source is in a low state, we find evidence for a flux variation on a period of 56.56 min. Although this period is close to twice the exposure time of the LC data, we consider it unlikely that this period is an artefact in the data. Since we can phase the SC data on a common ephemeris it strongly points to the fact that the 56.56 min period is a signature of the orbital period. As this period is below the short period minimum of hydrogen accreting CVs, BOKS 45906 may be a helium-rich CV. The *Kepler* light curve of BOKS 45906 provides a unique insight into the accretion history of a helium-rich CV over a 3 year time-scale. Phase-resolved spectroscopic observations of BOKS 45906 are required when the system is in a bright optical state to verify that the 56.56 min period is the orbital period.

ACKNOWLEDGEMENTS

Kepler was selected as the 10th mission of the Discovery Program. Funding for this mission is provided by NASA, Science Mission Directorate. The *Kepler* data presented in this paper were obtained from the Multimission Archive at the Space Telescope Science Institute (MAST). STScI is operated by the Association of Universities for Research in Astronomy, Inc., under NASA contract NAS5 26555. Support for MAST for non-*HST* data is provided by the NASA Office of Space Science via grant NAG5 7584 and by other grants and contracts. We acknowledge support via NASA's *Kepler* Grants 10-KEPLER10-0013 and 11-KEPLER11-0038. SH, SS and DG wish to thank Carolyn Heffner and Jean Mueller for their help and expertise at the 200 inch Hale Telescope during our observations. Armagh Observatory is supported by the Northern Ireland Government through the Department of Culture Arts and Leisure.

REFERENCES

Breedt E., Gänsicke B. T., Marsh T. R., Steeghs D., Drake A. J., Copperwheat C. M., 2012, MNRAS, 425, 2548
Burrows D. N. et al., 2005, Space Sci. Rev., 120, 165
Cannizzo J. K., 2012, ApJ, 757, L174
Carter P. J. et al., 2013, MNRAS, 431, 372
Drew J. E. et al., 2005, MNRAS, 362, 753
Feldmeier J. J. et al., 2011, AJ, 142, 2
Gänsicke B. T. et al., 2009, MNRAS, 397, 2170
Gehrels N. et al., 2004, ApJ, 611, 1005
Gies D. R. et al., 2013, ApJ, 775, 64
Greiss S. et al., 2012a, AJ, 144, 24
Greiss S. et al., 2012b, preprint (arXiv:1212.3613)
Groot P. J. et al., 2009, MNRAS, 399, 323
Howell S. B., Nelson L. A., Rappaport S., 2001, ApJ, 550, 897
Howell S. B. et al., 2013, AJ, 145, 109
Kato T., Maehara H., 2013, PASJ, 65, 76
Kinemuchi K., Barclay T., Fanelli M., Pepper J., Still M., Howell S. B., 2012, PASP, 124, 963
Kolb U., Baraffe I., 1999, MNRAS, 309, 1034
Osaki Y., Kato T., 2013, PASJ, 65, 50
Patterson J. P. et al., 2002, PASP, 114, 721
Ramsay G., Cannizzo J. K., Howell S. B., Wood M. A., Still M., Barclay T., Smale A., 2012, MNRAS, 425, 1479
Ramsay G. et al., 2013, MNRAS, preprint (arXiv:1310.0264)
Rappaport S., Joss P. C., Webbink R. F., 1982, ApJ, 254, 616
Roming P. W. A., 2005, Space Sci. Rev., 120, 95
Scaringi S., Groot P. J., Still M., 2013, MNRAS, 435, L68
Thorstensen J R., Fenton W. H., Patterson J. O., Kemp J., Krajci T., Baraffe I., 2002, ApJ, 567, L49
Voges W. et al., 1999, A&A, 349, 389

This paper has been typeset from a TEX/LATEX file prepared by the author.

Downloaded from http://mnras.oxfordjournals.org/ at NASA Goddard Space Flight Ctr on September 5, 2014